JOURNAL OF MATERIALS SCIENCE **40** (2005) 6433–6438

Study on novel antibacterial high-impact polystyrene/TiO_2 nanocomposites

ZHAOBO WANG*, GUICUN LI, HONGRUI PENG, ZHIKUN ZHANG
College of Material & Environment, Qingdao University of Science & Technology, No. 53 Zhengzhou Road, Qingdao 266042, People's Republic of China
E-mail: wangzhb@qingdaonews.com

XIN WANG
Key Laboratory of Rubber-Plastics, Ministry of Education, No. 53 Zhengzhou Road, Qingdao 266042, People's Republic of China

Published online: 5 October 2005

TiO_2 nanoparticles were introduced into High-impact polystyrene (HIPS) in the form of master batch where TiO_2 was pre-dispersed in HIPS by melt compounding. The microstructures and properties of the nanocomposites were investigated. Energy dispersive X-ray spectrometer (EDS) composition distribution maps indicate that TiO_2 nanoparticles are dispersed randomly in the nanocomposites comprising low TiO_2 content ($\leq$2wt.%), while the dispersion is inferior at high TiO_2 content. The variation in the dispersion behavior influences the mechanical properties of nanocomposites. Significantly, the surface of nanocomposites shows a strong absorption of UV light in the wavelength range of 250$\sim$400 nm, an increase in the TiO_2 content of nanocomposites raises the absorbance in the region. HIPS/TiO_2 nanocomposites have a satisfactory antibacterial effect on Escherichia coli(E. coli) and Staphylococcus aureus (S. aureus).

1. Introduction

With the increasing concern about health and safety, the sterilization of polymer products has assumed industrial importance. Products made from plastics, resins, or fibers are usually sterilized using dry/wet heat, ethylene oxide, or ionizing radiation. However, these products can still be contaminated or infected by microorganisms when exposed to air. The growth of microorganisms on the surface of polymers will inevitably increase the risk of transmitting infections. Polymers may also be invaded by bacteria or fungi, resulting in a loss of mechanical strength and the deterioration in appearance. The most common method for preventing the colonization of polymer from microorganisms is to add antibacterial agent into matrix during melt compounding [1]. Another method is to adopt polymers that have intrinsic antibacterial activity. Antibacterial polymers can be obtained by blending, grafting [2, 3], halogenation [4], and copolymerization [5]. Of these methods, blending is the most convenient, making it the most attractive to industry application.

During the process of melt compounding, inorganic fillers are generally introduced into the polymers as the antibacterial agent [6 ,7]. These agents are based on metal ions associated with materials such as TiO_2 [8] or zeolites [9]. The dispersion of antibacterial agent in matrix can confer a continuous, long lasting antibacterial activity on the surface of polymer. Of these agents, the antibacterial mechanism of TiO_2 has been thoroughly investigated. TiO_2 is a semiconductor photocatalyst that will generate hydroxyl radicals (OH·) on exposure to light, which plays an important role in the catalysis reaction [10]. The antibacterial function of TiO_2 comes from the high reactivity of the excited hydroxyl radicals. Linsebigler *et al*. shows that smaller semiconductor particles will increase the surface area and the catalytic effect [11]. Therefore, TiO_2 nanoparticles have better antibacterial activity than micron-sized particles.

High-impact polystyrene (HIPS) is a typical thermoplastic that is widely used in packaging, toys, bottles, housewares, electronic appliances, and light-duty industrial components because of its rigidity and ease of coloring and processing. In this study, we successfully prepared antibacterial HIPS/TiO_2 nanocomposites by melt compounding. Experimental characterization indicates the random dispersion of TiO_2 nanoparticles in HIPS matrix. The influences of TiO_2 nanoparticles on the other properties of the nanocomposites, such as the rheological behavior, UV/Vis absorbance, and mechanical properties, are also discussed.

*Author to whom all correspondence should be addressed.
0022-2461
DOI: 10.1007/s10853-005-1713-5

2. Experimental

2.1. Materials and sample preparation

HIPS, 466F type, was commercially obtained from Yangzi-BASF Company,China, with MFI of 4.80 g/10 min (5.0 kg at 200°C). TiO_2 nanoparticles (Qingdao Haier-QUST Nano Technology Research Co. Ltd., China) with average diameter of 80 nm were anatase phase.

2.2. Preparation of HIPS/TiO_2 nanocomposites

The HIPS/TiO_2 nanocomposites were prepared by a two-step melt compounding technique. HIPS and TiO_2 nanoparticles were dried for 8 h at 80°C and 100°C, respectively, before melt compounding. Firstly, the nanoparticles were mixed with HIPS at a weight ratio of 1**:**4; and then the mixture was granulated using a Brabender two-screw extruder (ZKS-25, Krupp Werner & Pfleiderer Gmbh, Germany) at 200°C.The as-prepared HIPS/TiO_2 master batch comprising 20 wt.% TiO_2 was diluted with HIPS by further melt compounding to obtain nanocomposites comprising the desired TiO_2 content. The nanocomposites pellets produced by the two-step melt compounding were fabricated into standard testing bars using an injection-molding machine (model J110EL-β). The barrel temperature was set at 200°C and the mold temperature at 40°C.

2.3. Characterization

2.3.1. Rheological analysis

The rheological behavior of the nanocomposites was measured with a Rosand Precision Rheometer (Bohlin Instruments, UK), in double-bore mode, with a capillary L/D ratio of 16**:**1. The experiments were carried out at 200°C. The experimental results were processed using Bohlin Instruments software, and all the rheological data obtained were subjected to Bagley and Rabinowitch calibration.

2.3.2. Titanium (Ti) element distribution analysis

The dispersion of TiO_2 nanoparticles on the surface of nanocomposites was indirectly measured by energy-dispersive X-ray microanalysis system (Oxford Instrument, U.K.). Before EDS imaging, the samples were sputtered with thin layers of gold.

2.3.3. UV-vis spectrum

The UV-Vis spectrum of specimens was studied using an ultraviolet-visible light spectrometer (Cary 500, Varian Instruments, USA).

2.3.4. Mechanical experiments

Notched specimens were tested with an API impact tester (Atlas Electric Devices Company, USA) according to the ISO 179 standard. The tests were carried out at room temperature, and the data obtained represent the average value from eight test specimens. Room temperature tensile testing was conducted on a H10KS-0282 universal testing machine (Hounsfield Test Equipment, UK) according to the ISO 527 standard at a crosshead speed of 10 mm/min. Five specimens were tested for each sample.

2.3.5. Antibacterial effect

Bactericidal activity was evaluated by examining the killing rate of Escherichia coli (E. coli) and Staphylococcus aureus (S. aureus) using the viable cell counting technique. The 40×40-mm square specimens of nanocomposites were firstly disinfected with a 75% ethanol solution. The concentrations of E. coli and S. aureus bacteria used here were both 10^6 colony forming units (cfu)/ml. The bacterial culture (0.2 ml) was transferred onto the surface of the specimens and then covered with a nontoxic 0.01-mm polyethylene (PE) film of the same size, to ensure even distribution of the bacterial solution on the surface of specimens. Later, the specimens were placed in a sterilized tank at 36°C and 90% relative humidity. The samples were irradiated with a 5 Watt daylight lamp. A comparison culture dish where pure HIPS specimen was placed was subjected to the same treatment. After stated time, the surfaces of the specimen and PE film were flushed with quantitative physiological saline, and several decimal dilutions were made. The surviving bacteria in the diluted solution was counted using the spread plate method. The difference between the number of surviving viable cells on the antibacterial nanocomposite specimen and that on the comparison culture dish was first calculated out, the ratio of this difference to the number of surviving viable cells on the comparison culture dish was defined as the antibacterial effect.

3. Results and discussion

3.1. Rheological properties of HIPS/TiO_2 nanocomposites

Two main factors affect the rheological behavior of the polymer/inorganic nanoparticles composites. The well-dispersed inorganic nanoparticles increase the free volume of the composites, which will lead to a decrease in apparent viscosity. This induced increase in free volume was first reported in rigid polymer/MMT composites [12], and was confirmed in our HIPS/TiO_2 system using the change in the glass transition temperature [13]. By contrast, if the melt of the nanocomposites is regarded as a suspending system, the volume effect induced by the filler can increase the melt viscosity. These two effects will influence the rheological behavior of the nanocomposites simultaneously.

The rheological behavior of HIPS/TiO_2 nanocomposites is plotted logarithmically in Fig. 1. All the melts exhibit typical pseudo-plastic behavior; the linear relationship between the apparent viscosity and shear rate is obvious. As shown, the rheological behavior is influenced only slightly by the variation in the TiO_2 content.

The apparent viscosity of the nanocomposites comprising 20 wt.% TiO_2 is slightly higher than that of pure HIPS. At lower TiO_2 content, the rheology curves almost overlap that of pure HIPS. Interestingly, when the shear rate exceeds 1,000 s^{-1}, the nanocomposite comprising 1 wt.% TiO_2 has a lower apparent viscosity than that of pure HIPS. This will be useful in the modeling process.

The rheometer software provides the non-Newtonian index at any shear rate. Fig. 2 shows the non-Newtonian index as a function of shear rate. The non-Newtonian index of HIPS decreases as the shear rate increases, as expected for a pseudo-plastic fluid. For the specimen comprising 20 wt.% TiO_2, the TiO_2 nanoparticles in composites significantly decreases the range of the non-Newtonian index, which remains nearly constant over the whole range of shear rates. By contrast, for the nanocomposite comprising 1 wt.% TiO_2, the variation in the non-Newtonian index is much greater than that of HIPS. In Fig. 2, there is an intersection point at a shear rate of 300 s^{-1}. At lower shear rates, the existence of TiO_2 in the nanocomposites comprising 1 wt.% TiO_2 increases the non-Newtonian index, whereas at higher rates it is decreased in comparison with HIPS system. This disparity is thought to result from the different dispersion conditions of TiO_2 nanoparticles in matrix. At low shear rates, TiO_2 nanoparticles are dispersed in the form of particle agglomerates. With increasing the shear rate, the TiO_2 agglomerates are gradually destroyed by the effect of shear. The reduction in the size of the dispersed units is accompanied by an increase in the inner free volume in the molecularly rigid HIPS, causing the abnormal behavior of the non-Newtonian indexes of the melt.

3.2. Dispersion of TiO_2 nanoparticles on the surface of nanocomposites

To date, most researchers have used transmission electron microscopy (TEM) to observe the dispersion morphology of nanoparticles at much high magnification. Only rarely are the nanoparticles dispersion investigated under low magnification by using other test approaches, such as energy dispersive X-ray spectrometer (EDS). Investigation of the TiO_2 content on the surface of the HIPS/TiO_2 nanocomposites is important in that the antibacterial effect is determined by the content and dispersion of TiO_2 on the surface of the specimens. Therefore, we used EDS to reveal the dispersion of TiO_2 nanoparticles on the surface of the composites at a lower resolution, but with a larger sampling area.

Fig. 3 shows EDS images of Ti element on the surface of the HIPS/TiO_2 nanocomposites. The white dots are the X radial signals radiated from Ti element. It is found that TiO_2 nanoparticles are randomly dispersed in the HIPS matrix, especially at lower TiO_2 contents (Fig. 3a). However, this uniformity disappears in the nanocomposites comprising a high TiO_2 content (Fig. 3c). EDS images show that the TiO_2 nanoparticles were well dispersed in the nanocomposites comprising low TiO_2 content as a result of two-step melt compounding. Therefore, we postulate that the antibacterial efficacy resulted from the good surface dispersion of TiO_2 nanoparticles.

3.3. UV/Vis spectra of HIPS/TiO_2 nanocomposites

Fig. 4 shows the UV/Vis spectra of the nanocomposites. The nanocomposites comprising a low TiO_2 content (1∼3 wt.%) show strong absorbance in the UV region and little absorbance at visible wavelengths as compared to HIPS. Obviously, the increase in the TiO_2 content of the nanocomposites raises the absorbance in the UV region significantly, especially from 250 to 350 nm. Therefore, TiO_2 nanoparticles on the surface of the nanocomposites will be excited by UV radiation and consequently exert an antibacterial effect. Interestingly, the absorbance in the visible region from 500 to 800 nm decreases with increasing TiO_2 content. This is attributed to the higher reflectivity of TiO_2 nanoparticles compared with the HIPS matrix in this region. With increasing TiO_2 content in nanocomposites, more TiO_2 nanoparticles will be distributed on the surface, lowering the absorbance of visible light, while increasing that of UV.

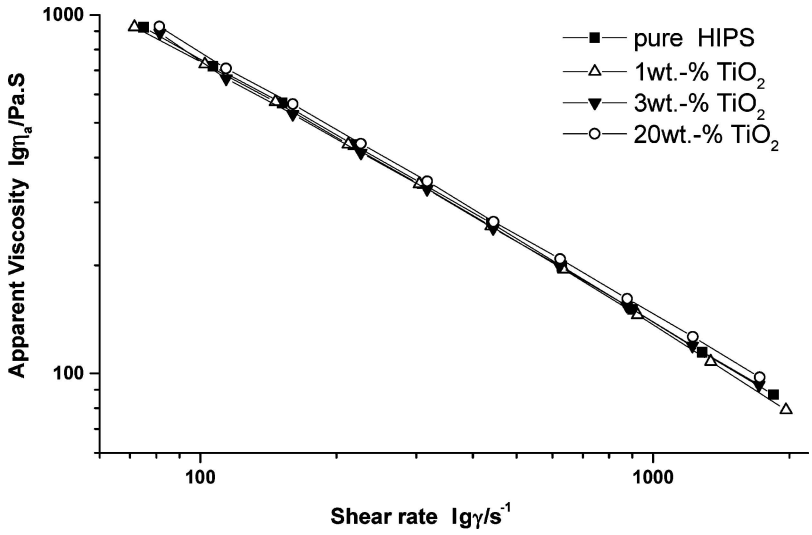

Figure 1 Rheological curves of HIPS/TiO_2 nanocomposites and HIPS.

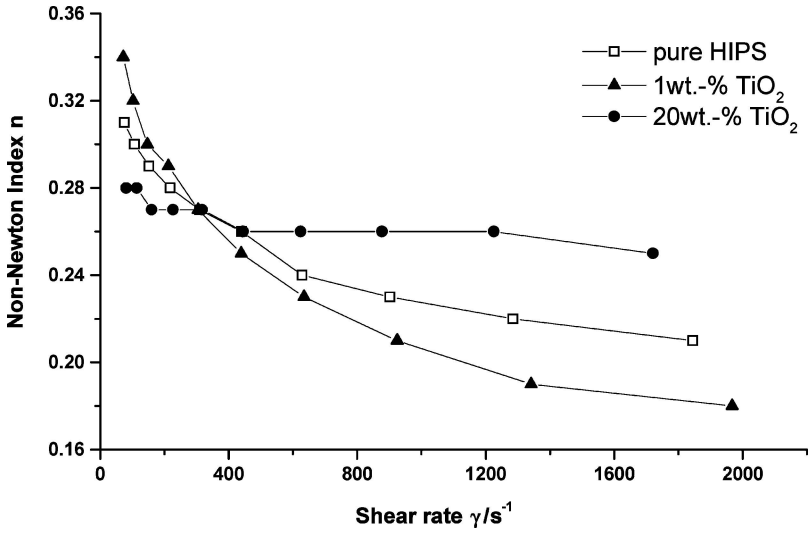

Figure 2 Dependence of the non-Newtonian indexes of HIPS/TiO_2 nanocomposites on shear rate.

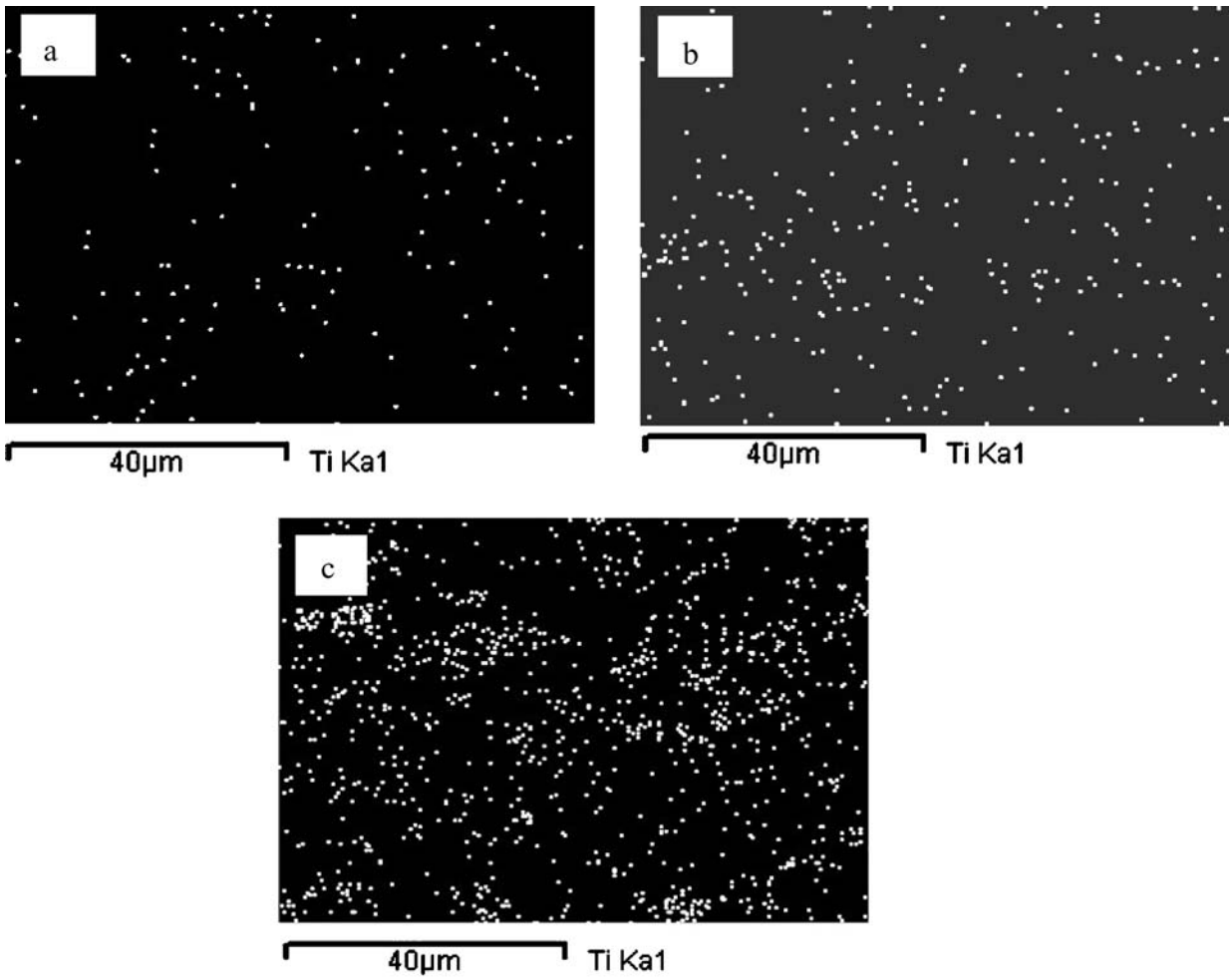

Figure 3 EDS composition distribution map of Ti element on the surface of nanocomposites comprising different TiO_2 contents (wt.%): (a) 1, (b) 2, (c) 3.

3.4. Mechanical properties

The relationship between the TiO_2 content and notched impact strength is shown in Fig. 5. The notched impact strength is maximal when the TiO_2 content is 1 wt.%, however the increase is not very significant compared with the experimental range. The influence of TiO_2 nanoparticle on the mechanical property of nanocomposites can be attributed to two factors according to its dispersion. First, the presence of well-dispersed nanoparticles within the matrix facilitates more plastic deformation than that in pure HIPS. As Nakagawa showed [14], this will increase the stress necessary to begin microcracks during the fracture of nanocomposites. The consequent plastic deformation around the nanoparticles will absorb more impact energy, achieving better impact strength from well-dispersed TiO_2.

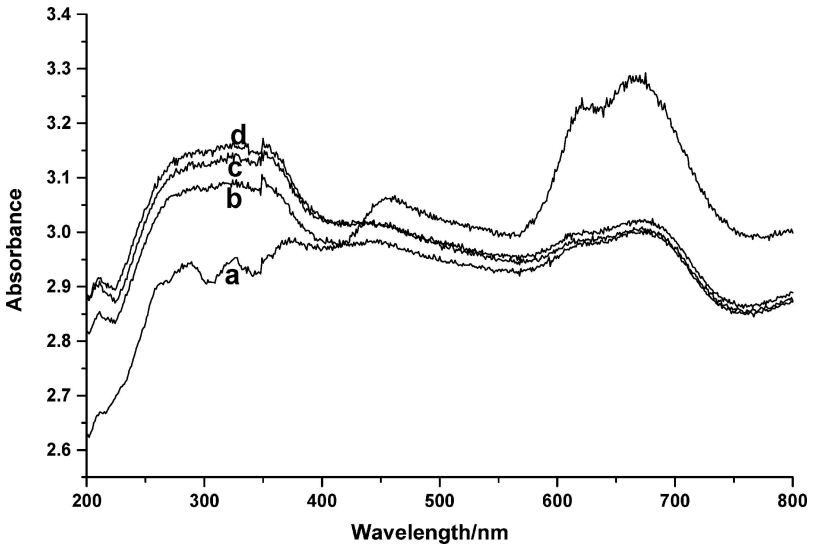

Figure 4 UV/Vis spectrum of HIPS/TiO_2 nanocomposites comprising different TiO_2 contents (wt.%): (a) pure HIPS, (b) 1, (c) 2, (d) 3.

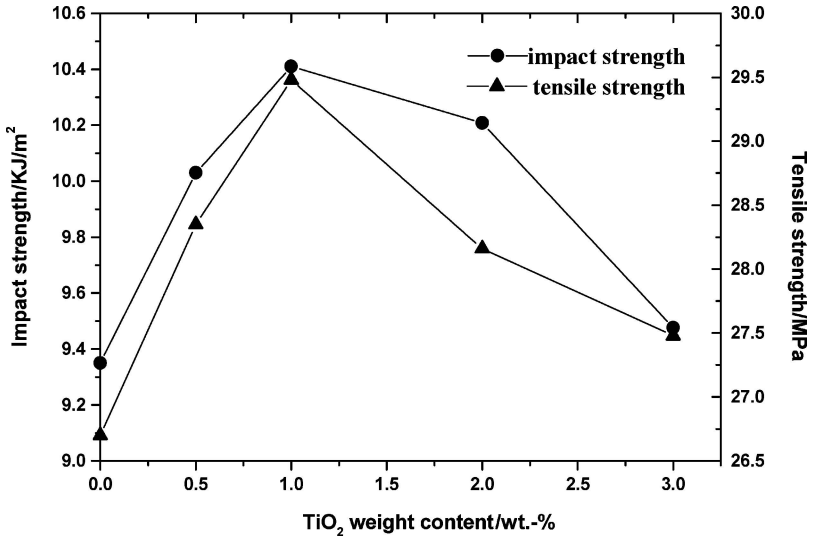

Figure 5 Effect of TiO_2 content on the mechanical properties of HIPS/TiO_2 nanocomposites.

However, when more nanoparticles are introduced into the HIPS matrix, the nanoparticles do not retain their uniform dispersion, even using two-step melt mixing. When TiO_2 is dispersed in the form of large agglomerates in the HIPS matrix, these will become the site of stress concentration and act to initiate microcracks, decreasing the notched impact strength [15]. Fig. 3 shows that TiO_2 nanoparticles are dispersed in HIPS as both separate particles and agglomerates. The dispersion of TiO_2 changs with the TiO_2 content, and the agglomerate content increases as more TiO_2 nanoparticles are introduced into the HIPS. Consequently, the impact strength peaks at a certain TiO_2 content, rather than increasing continuously.

The influence of TiO_2 on tensile strength is also shown in Fig. 5. The tensile strength of the nanocomposites is slightly higher than that of pure HIPS where the TiO_2 wt.% is 1–3% and reachs a maximum at 1 wt% TiO_2 content. Clearly, the influence of TiO_2 content on the tensile strength of the nanocomposites is similar to that on the impact strength, and the mechanism is analogous. When TiO_2 nanoparticles are randomly dispersed in the HIPS matrix, good interfacial adhesion will be formed. This increases the ability of the interfacial structure to bear part of the tensile strength inside the nanocomposites [16]. However, as the TiO_2 content increases, the agglomerates act as microcrack initiators, again reducing the tensile strength.

According to the analysis in Fig. 5, we can understand that at low TiO_2 content, TiO_2 nanoparticles are dispersed randomly in matrix via two-step melt compounding. Even without pre-treatment with a coupling agent, however,TiO_2 nanoparticles can enhance the mechanical properties of the nanocomposites.

3.5. Antibacterial assessment

The antibacterial effect of the prepared nanocomposites comprising 1 wt.% TiO_2 on E. coli and S. aureus is shown in Table I. We can know that the antibacterial effect after 12 hr contacting is relatively weak, however, the antibacterial effect increases remarkable with increasing contacting time to 24 h. This indicates the antibacterial effect of HIPS/TiO_2 nanocomposites is associated with contacting time obviously. Furthermore, the antibacterial mechanism of TiO_2

TABLE I The antibacterial effect of HIPS/TiO_2 nanocomposites (TiO_2 wt.% = 1)

	The antibacterial effects (%)			
Bacterium species	Contacting time	12 h	24 h	24 h*
E. coli		90.5	99.2	95.0
S. aureus		91.0	99.6	96.5

*The specimens have been carried out an antibacterial assessment 48 h before the experiment.

nanoparticles is based on photocatalytic activity and has no self-loss during the antibacterial process, Table 1 also shows that the specimen still have well antibacterial effect even shortly after antibacterial assessment, the slight decrease of antibacterial effect may be caused by the rejuvenation of photocatalytic activity. The systemic assessment of antibacterial effect under various conditions is in research.

4. Conclusion

In this study, antibacterial HIPS/TiO_2 nanocomposites were prepared by two-step melt compounding technique. We reach the following conclusions:

1. The introduction of TiO_2 nanoparticles influences the processability of HIPS slightly. At a low TiO_2 content, it appears to improve the rheological behavior. Further analysis indicates that this is owing to further dispersion of TiO_2 nanoparticles induced by shear.
2. At low magnification, EDS reveals that melt compounding resulted in the random dispersion of the Ti on the surface at low TiO_2 content ($\leq$2 wt.%).
3. The surface of HIPS/TiO_2 nanocomposites can absorb UV light strongly with the wavelength from 250 to 400 nm. The UV absorption increases with the loading of TiO_2, while the reflection of visual light is significantly improved by introducing TiO_2.
4. Assessment of specimens comprising 1 wt.% TiO_2 shows that the nanocomposites exhibit satisfactory antibacterial effects against E. coli and S. aureus.

References

1. G. SAUVET, S. DUPOND and K. KAZMIERSKI, *J. Appl. Polym. Sci.* **75** (2000) 1005.
2. S. P. JONG, H. K. JAE and C. N. YOUNG, *ibid.* **69** (1998) 2213.
3. M. W. HUH, I. K. KANG and D. H. LEE, *ibid.* **81** (2001) 2769.
4. Y. SUN and G. SUN, *ibid.* **80** (2001) 2460.
5. A. KANAZAWA, T. IKEDA and T. ENDO, *ibid.* **53** (1994) 1245.
6. T. YAMAMOTO, S. UCHIDA, Y. KURHARA and I. NAKAYAMA, *Jpn. Pat.* 94-204681 (1994).
7. K. SUGIURA, H. INOUE, S. MAEKAWA, H. KATO and T. OMAURA, *Jpn. Pat.* 91-57823 (1991).
8. J. KELEHER, J. BASHANT, N. HELDT, L. JOHNSON and Y. Z. LI, *World J. Microbiol. Biotech.* **18** (2002) 133.
9. Y. INOUE, M. HOSHINO, H. TAKAHASHI, T. NOGUCHI, T. MURATA, Y. KANZAKI, H. HAMASHIMA and M. SASATSU, *J. Inorg. Biochem.* **92** (2002) 37.
10. P. V. KAMAT, *Chem. Rev.* **93** (1993) 267.
11. A. L. LINSEBIGLER, *ibid.* **95** (1995) 735.
12. J. LV, M. QIN, Y. KE, Z. QI and Y. XI, *Acta. Polym.Sinica.* **1** (2002) 73.
13. X. WANG, Z. B. WANG and Q. Y. WU, *J. Appl. Polym. Sci.* **96** (2005) 802.
14. H. NAKAGAWA and H. SANO, *Polym. Prep.* (*Am. Chem. Soc., Div. Polym. Chem.*) **26** (1992) 249.
15. P. MARERI, S. BASTIDE, N. BINDA and A. CRESPY, *Compos. Sci. Technol.* **58** (1998) 747.
16. S. W. SHANG, J. W. WILLIAMS and K. J. M. SODERHOLM, *J. Mater. Sci.* **29** (1994) 2406.

Received 14 January
and accepted 26 April 2005